



## **AIAA 2004–1096**

### **Adaptive precision methodology for flow optimization via discretization and iteration error control**

James Lu

David L. Darmofal

*Massachusetts Institute of Technology, Cambridge MA  
02139*

**42nd AIAA Aerospace Sciences  
Meeting and Exhibit  
January 5–8, 2004/Reno, NV**

# Adaptive precision methodology for flow optimization via discretization and iteration error control

James Lu\*

David L. Darmofal†

*Massachusetts Institute of Technology, Cambridge MA 02139*

**An adaptive precision optimization methodology based on discretization and iteration error estimates is presented. Issues of efficient concurrent flow-adjoint solution and consistency between PDE and discrete adjoint for the Discontinuous Galerkin (DG) discretization of the Euler compressible equations are developed. Optimization results for quasi-one dimensional channel flow are presented to demonstrate the methodology.**

## Introduction

The computational optimization of flows satisfying the governing differential systems of equations necessarily require some form of discretization. Furthermore, the fine discretizations needed for the accurate prediction of quantities to be optimized give rise to large nonlinear systems of algebraic equations, the approximate solutions of which are obtained through an iterative procedure. However, when the design is far from optimal, improvements in the design may be possible even with relatively coarse discretizations. A desirable approach for computational optimization would require only enough discretization accuracy to guarantee that the performance of the modified design has improved. Similarly, the iterative solution process may be controlled by requiring convergence only to the level necessary to determine if the design has improved. In this paper, we present a framework for optimization in which the discretization and iteration errors present in the objective function are adaptively controlled allowing significant reduction in the overall computational cost of optimization.

The adaptive precision optimization algorithm we propose is based on an approach developed by Polak et al.<sup>1,2</sup> Whereas Polak et al utilize a priori error estimates to control the adaptive precision algorithm, we rely on the a posteriori error estimates for the objective function arising from both discretization and incomplete iteration. A framework for the a posteriori estimation of output errors due to discretization exists within the finite element community.<sup>3,4</sup> We show that

a similar strategy can be used to estimate the error due to incomplete iteration and that by including this iteration error estimate, the output converges (iteratively) at twice the rate of the residual.

In this work, we employ a high-order Discontinuous Galerkin (DG) discretization of the compressible flow equations.<sup>5-7</sup> We demonstrate that by suitably formulating the primal boundary conditions and the output functional, the discrete adjoint of the DG flow discretization is identical to a DG discretization of the continuous adjoint problem. Thus, the same discrete adjoint solution used for the evaluation of the objective function gradient in the optimization process may be directly used to estimate both the discretization and iterative error.

Traditionally, the adjoint solution is iterated after the flow solution has converged. In this paper, we propose to iterate the flow and adjoint solutions concurrently. Thus, the linearization that produces the adjoint equations is about a different primal state at every iteration and must be continually re-evaluated. However, since the linearization is already being re-evaluated as part of the flow solution algorithm, the concurrent iteration of the adjoint problem adds only a minor computational cost compared to the flow solution itself. As a result, the overall flow-adjoint solution process is significantly more effective when performed concurrently as opposed to sequentially.

The paper begins with a description of the DG discretization of the two-dimensional compressible Euler equations. Then, we consider the relationship between the continuous adjoint and the discrete adjoint for the DG method. Next, we describe our concurrent flow-adjoint iterative algorithm and the error estimate due to incomplete iteration. Finally, we present the adaptive precision optimization method and give preliminary results for the simpler quasi-one dimensional channel flow setting.

---

\*Graduate research assistant. Email : jameslu@mit.edu

†Associate Professor, Senior Member AIAA. 77 Massachusetts Ave. 37-401, Cambridge, MA 02139. Ph. (617) 258-0743. Email: darmofal@mit.edu.

Copyright © 2004 by the American Institute of Aeronautics and Astronautics, Inc. No copyright is asserted in the United States under Title 17, U.S. Code. The U.S. Government has a royalty-free license to exercise all rights under the copyright claimed herein for Governmental Purposes. All other rights are reserved by the copyright owner.

## Discretization

The equations for two-dimensional compressible Euler flow are given by,

$$\frac{\partial \mathbf{F}^x(\mathbf{u})}{\partial x} + \frac{\partial \mathbf{F}^y(\mathbf{u})}{\partial y} = 0, \quad \mathbf{x} \in \Omega, \quad (1)$$

where  $\mathbf{u}$  is the conservative state vector,

$$\mathbf{u} = \begin{pmatrix} \rho \\ \rho u \\ \rho v \\ \rho E \end{pmatrix},$$

and the inviscid fluxes are,

$$\mathbf{F}^x = \begin{pmatrix} \rho u \\ \rho u^2 + p \\ \rho uv \\ \rho u H \end{pmatrix}, \quad \mathbf{F}^y = \begin{pmatrix} \rho v \\ \rho uv \\ \rho v^2 + p \\ \rho v H \end{pmatrix}.$$

The total enthalpy is given by  $H = E + p/\rho$ . In addition, we have the equation of state,

$$p = (\gamma - 1) \left[ \rho E - \frac{1}{2} \rho (u^2 + v^2) \right].$$

On  $\partial\Omega$ , Dirichlet boundary conditions are imposed, denoted as  $\text{DirichBC}(\mathbf{u}|_{\partial\Omega}) = 0$ . Denote  $\mathcal{V}_h^p$  to be the space of discontinuous vector-valued polynomials of degree  $p$  on a subdivision  $T_h$  of domain  $\Omega$  into elements such that  $\bar{\Omega} = \bigcup_{\kappa \in T_h} \bar{\kappa}$ . The DG discretization of the Euler equations is of the form: find  $\mathbf{u}_h \in \mathcal{V}_h^p$  such that  $\forall \mathbf{v}_h \in \mathcal{V}_h^p$ ,

$$\begin{aligned} & \sum_{\kappa \in T_h} \left\{ - \int_{\kappa} \mathcal{F}(\mathbf{u}_h) \cdot \nabla \mathbf{v}_h dx \right. \\ & + \int_{\partial\kappa \setminus \partial\Omega} \mathcal{H}(\mathbf{u}_h^+, \mathbf{u}_h^-, \hat{\mathbf{n}}) \mathbf{v}_h^+ ds \\ & \left. + \int_{\partial\kappa \cap \partial\Omega} \mathcal{H}_{\text{bd}}(\mathbf{u}_h^+, \mathbf{u}_h^-, \hat{\mathbf{n}}) \mathbf{v}_h^+ ds \right\} = 0, \quad (2) \end{aligned}$$

where on  $\partial\kappa$ ,  $\hat{\mathbf{n}}$  is the outward pointing normal and  $(\cdot)^+$  and  $(\cdot)^-$  are the interior and exterior traces respectively with respect to element  $\kappa$ ;  $\mathcal{F}(\mathbf{u}_h) \equiv [\mathbf{F}^x(\mathbf{u}_h), \mathbf{F}^y(\mathbf{u}_h)]$ ,  $\mathcal{H}(\mathbf{u}_h^+, \mathbf{u}_h^-, \hat{\mathbf{n}})$  are inviscid and (an arbitrary) numerical flux functions respectively. The numerical flux function  $\mathcal{H}_{\text{bd}}(\mathbf{u}_h^+, \mathbf{u}_h^-, \hat{\mathbf{n}})$  used to evaluate the boundary flux on  $\partial\Omega$  need not coincide with that used for the interior edges. The boundary conditions on  $\partial\Omega$  are imposed weakly through constructing an exterior boundary state on  $\partial\Omega$  that is a function of the inner state and BC data,  $\mathbf{u}_h^-(\mathbf{u}_h^+, \text{BCData})$ .

## Regularity of discrete adjoint

In aerodynamic applications, the inflow and outflow boundary condition (BC) are typically set by specifying quantities such as  $T_t, p_t, p$ . In the weak enforcement of these BC's, the characteristics from the interior of the flow domain are combined with these set quantities to construct exterior states at the domain boundary. The dependence of the boundary flux and output on the interior and constructed states affects the regularity of the corresponding discrete adjoint problems. In the work of Hartmann and Houston,<sup>8</sup> it is noted that the adjoint solution for the subsonic flow around the NACA0012 airfoil large gradients near the airfoil surface.

We show that by appropriate weak BC enforcement, this lack of regularity can be removed. More specifically, for the discrete adjoint to be consistent with the PDE adjoint, the boundary flux and output should depend only on the constructed but not the interior states. In doing so, the numerically introduced singularities in the discrete adjoint solution do not appear. Moreover, we demonstrate that this is also a necessary condition for obtaining output superconvergence naturally present in the Galerkin discretization.

With  $\mathbf{u}$  the solution to the flow equations (1) with Dirichlet condition denoted as  $\text{DirichBC}(\mathbf{u}|_{\partial\Omega}) = 0$ , the PDE system for adjoint state  $\psi$  associated to the output  $\mathcal{J}(\mathbf{u}) \equiv \int_{\Gamma_{\text{output}}} J(\mathbf{u}) ds$ ,  $\Gamma_{\text{output}} \subset \partial\Omega$ , satisfies the following,<sup>9</sup>

$$- \left[ \frac{d\mathbf{F}^x}{d\mathbf{u}} \right]^T \frac{\partial \psi}{\partial x} - \left[ \frac{d\mathbf{F}^y}{d\mathbf{u}} \right]^T \frac{\partial \psi}{\partial y} = 0, \quad \mathbf{x} \in \Omega, \quad (3)$$

subject to:

$$\begin{aligned} & \int_{\partial\Omega} \left( n_x \left[ \frac{d\mathbf{F}^x}{d\mathbf{u}} \right] \tilde{\mathbf{u}} + n_y \left[ \frac{d\mathbf{F}^y}{d\mathbf{u}} \right] \tilde{\mathbf{u}} \right) \psi ds \\ & = \int_{\Gamma_{\text{output}}} \frac{dJ(\mathbf{u})}{d\mathbf{u}} \tilde{\mathbf{u}} ds, \\ & \forall \tilde{\mathbf{u}} \in \{ \tilde{\mathbf{u}} \mid \text{DirichBC}(\tilde{\mathbf{u}}|_{\partial\Omega}) = 0 \}. \quad (4) \end{aligned}$$

That is, the adjoint BC is formulated to remove the dependence of the boundary terms and the output on  $\tilde{\mathbf{u}}$  for all variations  $\tilde{\mathbf{u}}$  satisfying the flow Dirichlet BC. Hence, components of variations  $\tilde{\mathbf{u}}$  allowed by the flow Dirichlet data give rise to BC's for  $\psi$ , whereas components of  $\tilde{\mathbf{u}}$  fixed by the Dirichlet data do not give rise to restraints for  $\psi$ . When the flow problem is discretized and the discrete adjoint is taken, the resulting adjoint satisfies a BC that is implicitly given by both the manner the flow BC is set and how the output is computed. For the discrete adjoint to have the same regularity as the PDE adjoint, the boundary conditions need to be in correspondence.

The discrete adjoint bilinear form is obtained by linearizing (2) and permuting the test and trial func-

tions. Hence, for a given functional supported on  $\Gamma_{\text{output}} \subset \partial\Omega$  with the general dependence on interior and exterior traces,  $\mathcal{J}(\mathbf{u}_h) \equiv \int_{\Gamma_{\text{output}}} J_h(\mathbf{u}_h^+, \mathbf{u}_h^-) ds$ , the discrete adjoint problem is: find  $\boldsymbol{\psi}_h \in \mathcal{V}_h^p$  such that  $\forall \mathbf{v}_h \in \mathcal{V}_h^p$ ,

$$\begin{aligned} & \sum_{\kappa \in T_h} \left\{ - \int_{\kappa} \left( \frac{d\mathcal{F}(\mathbf{u}_h)}{d\mathbf{u}_h} \mathbf{v}_h \right) \cdot \nabla \boldsymbol{\psi}_h dx \right. \\ & + \int_{\partial\kappa \setminus \partial\Omega} \left( \frac{\partial \mathcal{H}(\mathbf{u}_h^+, \mathbf{u}_h^-, \hat{\mathbf{n}})}{\partial \mathbf{u}_h^+} \mathbf{v}_h^+ \right. \\ & \quad \left. + \frac{\partial \mathcal{H}(\mathbf{u}_h^+, \mathbf{u}_h^-, \hat{\mathbf{n}})}{\partial \mathbf{u}_h^-} \mathbf{v}_h^- \right) \boldsymbol{\psi}_h^+ ds \\ & + \int_{\partial\kappa \cap \partial\Omega} \left( \frac{\partial \mathcal{H}_{\text{bd}}(\mathbf{u}_h^+, \mathbf{u}_h^-, \hat{\mathbf{n}})}{\partial \mathbf{u}_h^+} \mathbf{v}_h^+ \right. \\ & \quad \left. + \frac{\partial H_{\text{bd}}(u_h^+, u_h^-, \hat{\mathbf{n}})}{\partial \mathbf{u}_h^-} \left[ \frac{d\mathbf{u}_h^-}{d\mathbf{u}_h^+} \right] \mathbf{v}_h^+ \right) \boldsymbol{\psi}_h^+ ds \left. \right\} \\ & = \int_{\Gamma_{\text{output}}} \left( \frac{\partial J_h(\mathbf{u}_h^+, \mathbf{u}_h^-)}{\partial \mathbf{u}_h^+} \mathbf{v}_h^+ \right. \\ & \quad \left. + \frac{\partial J_h(\mathbf{u}_h^+, \mathbf{u}_h^-)}{\partial \mathbf{u}_h^-} \left[ \frac{d\mathbf{u}_h^-}{d\mathbf{u}_h^+} \right] \mathbf{v}_h^+ \right) ds. \end{aligned}$$

Consider test function variations supported on an interior element  $\kappa$ ,  $\bar{\kappa} \cap \partial\Omega = \emptyset$ . Making use of the conservative property  $\mathcal{H}(\mathbf{u}, \mathbf{v}, \hat{\mathbf{n}}) = -\mathcal{H}(\mathbf{v}, \mathbf{u}, -\hat{\mathbf{n}})$ , the above implies that  $\forall \mathbf{v}_h \in \mathcal{V}_h^p|_{\kappa}$ :

$$\begin{aligned} & - \int_{\kappa} \left( \frac{d\mathcal{F}(\mathbf{u}_h)}{d\mathbf{u}_h} \mathbf{v}_h \right) \cdot \nabla \boldsymbol{\psi}_h dx \\ & + \int_{\partial\kappa} \left( \left[ \frac{\partial \mathcal{H}(\mathbf{u}_h^+, \mathbf{u}_h^-, \hat{\mathbf{n}})}{\partial \mathbf{u}_h^+} \right]^T (\boldsymbol{\psi}_h^+ - \boldsymbol{\psi}_h^-) \right) \mathbf{v}_h^+ ds \\ & = 0. \end{aligned} \quad (5)$$

Thus, an inter-element adjoint flux exists which depends on the adjoint jump  $\boldsymbol{\psi}_h^+ - \boldsymbol{\psi}_h^-$ .

On  $\partial\Omega$ , possible choices for the functional dependence of the numerical flux  $\mathcal{H}_{\text{bd}}$  on the state include: both the interior state  $\mathbf{u}_h^+$  and the constructed exterior state,  $\mathbf{u}_h^-(\mathbf{u}_h^+, \text{BCData})$ ; or just  $\mathbf{u}_h^-(\mathbf{u}_h^+, \text{BCData})$ . Similarly, several choices exist for the output. These give rise to different discrete BC's for the adjoint. Some of these cases are examined below, by considering an element  $\kappa$  whose closure intersects the boundary,  $\bar{\kappa} \cap \partial\Omega \neq \emptyset$ .

**Boundary flux and output:**  $\mathcal{H}_{\text{bd}}(\mathbf{u}_h^-)$ ,  $J_h(\mathbf{u}_h^-)$

On an element  $\kappa$  intersecting the boundary, the discrete adjoint satisfies  $\forall \mathbf{v}_h \in \mathcal{V}_h^p|_{\kappa}$ ,

$$\begin{aligned} & - \int_{\kappa} \left( \frac{d\mathcal{F}(\mathbf{u}_h)}{d\mathbf{u}_h} \mathbf{v}_h \right) \cdot \nabla \boldsymbol{\psi}_h dx + \int_{\partial\kappa \setminus \partial\Omega} \left( \left[ \frac{\partial \mathcal{H}(\mathbf{u}_h^+, \mathbf{u}_h^-, \hat{\mathbf{n}})}{\partial \mathbf{u}_h^+} \right]^T (\boldsymbol{\psi}_h^+ - \boldsymbol{\psi}_h^-) \right) \mathbf{v}_h^+ ds \\ & + \int_{\partial\kappa \cap \partial\Omega} \left( \left[ \frac{d\mathcal{H}_{\text{bd}}(\mathbf{u}_h^-(\mathbf{u}_h^+, \text{BCData}), \hat{\mathbf{n}})}{d\mathbf{u}_h^-} \frac{d\mathbf{u}_h^-}{d\mathbf{u}_h^+} \right]^T \boldsymbol{\psi}_h^+ \right) \mathbf{v}_h^+ ds \end{aligned}$$

$$= \int_{\partial\kappa \cap \Gamma_{\text{output}}} \frac{dJ_h(\mathbf{u}_h^-(\mathbf{u}_h^+, \text{BCData}))}{d\mathbf{u}_h^-} \frac{d\mathbf{u}_h^-}{d\mathbf{u}_h^+} \mathbf{v}_h^+ ds.$$

Hence, for the set of variations fixed by the flow BC,  $\mathbf{v}_h : [d\mathbf{u}_h^-/d\mathbf{u}_h^+] \mathbf{v}_h = 0$ , only the first two terms of (6) remain. The absence of terms supported on  $\partial\kappa \cap \partial\Omega$  is consistent with not setting adjoint BC for primal state variations fixed by the BC data.

For the set of allowed flow state variations,  $\mathbf{v}_h \in \text{range}([d\mathbf{u}_h^-/d\mathbf{u}_h^+])$ , the discrete adjoint BC corresponds to a finite dimensional equivalence of the PDE adjoint BC (4) assuming  $\mathcal{H}_{\text{bd}}(\mathbf{u}_h^-) = \mathcal{F}^{\hat{\mathbf{n}}}(\mathbf{u}_h^-)$ .

**Boundary flux and output:**  $\mathcal{H}_{\text{bd}}(\mathbf{u}_h^+, \mathbf{u}_h^-)$ ,  $J_h(\mathbf{u}_h^-)$

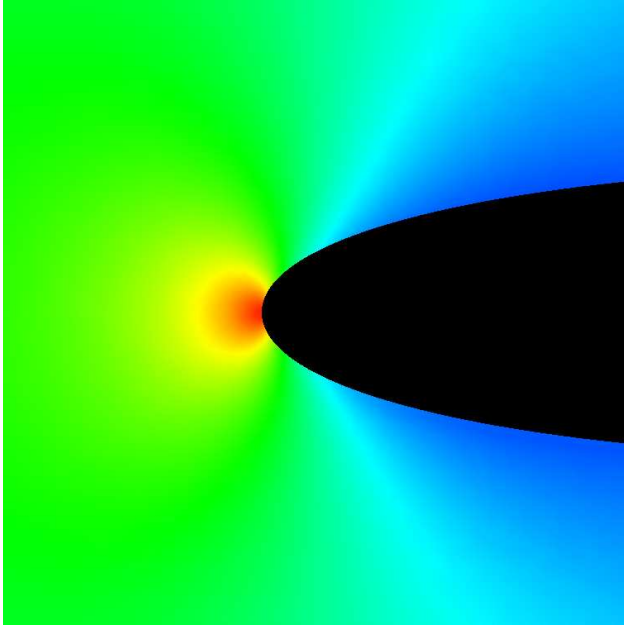
$$\begin{aligned} & - \int_{\kappa} \left( \frac{d\mathcal{F}(\mathbf{u}_h)}{d\mathbf{u}_h} \mathbf{v}_h \right) \cdot \nabla \boldsymbol{\psi}_h dx \\ & + \int_{\partial\kappa \setminus \partial\Omega} \left( \left[ \frac{\partial \mathcal{H}(\mathbf{u}_h^+, \mathbf{u}_h^-, \hat{\mathbf{n}})}{\partial \mathbf{u}_h^+} \right]^T (\boldsymbol{\psi}_h^+ - \boldsymbol{\psi}_h^-) \right) \mathbf{v}_h^+ ds \\ & + \int_{\partial\kappa \cap \partial\Omega} \left( \left[ \frac{\partial \mathcal{H}_{\text{bd}}(\mathbf{u}_h^+, \mathbf{u}_h^-(\mathbf{u}_h^+, \text{BCData}), \hat{\mathbf{n}})}{\partial \mathbf{u}_h^+} \right. \right. \\ & \quad \left. \left. + \frac{\partial \mathcal{H}_{\text{bd}}(\mathbf{u}_h^+, \mathbf{u}_h^-(\mathbf{u}_h^+, \text{BCData}), \hat{\mathbf{n}})}{\partial \mathbf{u}_h^-} \frac{d\mathbf{u}_h^-}{d\mathbf{u}_h^+} \right]^T \boldsymbol{\psi}_h^+ \right) \mathbf{v}_h^+ ds \\ & = \int_{\partial\kappa \cap \Gamma_{\text{output}}} \frac{dJ_h(\mathbf{u}_h^-(\mathbf{u}_h^+, \text{BCData}))}{d\mathbf{u}_h^-} \frac{d\mathbf{u}_h^-}{d\mathbf{u}_h^+} \mathbf{v}_h^+ ds. \end{aligned}$$

For  $\mathbf{v}_h : [d\mathbf{u}_h^-/d\mathbf{u}_h^+] \mathbf{v}_h = 0$ , there exists the generally non-zero term coming from the inner-product of  $[\partial \mathcal{H}_{\text{bd}}/\partial \mathbf{u}_h^+]^T \boldsymbol{\psi}_h^+$  with  $\mathbf{v}_h^+$  over  $\partial\kappa \cap \partial\Omega$ . However, there is no other inter-element flux term with the same support. The result is equivalent to weakly setting  $\boldsymbol{\psi}_h^+$  so that  $[\partial \mathcal{H}_{\text{bd}}/\partial \mathbf{u}_h^+]^T \boldsymbol{\psi}_h^+ = 0$  over this space of  $\mathbf{v}_h$ . Hence if  $[d\mathbf{u}_h^-/d\mathbf{u}_h^+]$  has a nonempty null-space, this formulation will introduce adjoint BC's not present in the corresponding PDE problem and introducing irregularities at the boundaries.

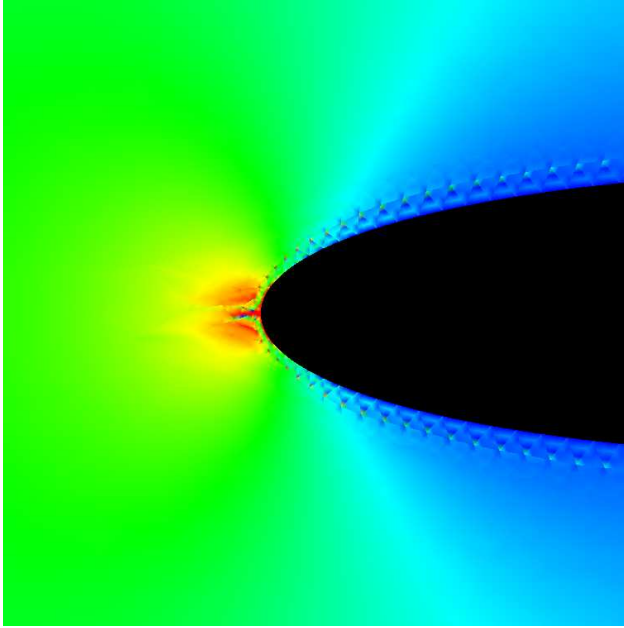
**Boundary flux and output:**  $\mathcal{H}_{\text{bd}}(\mathbf{u}_h^+, \mathbf{u}_h^-)$ ,  $J_h(\mathbf{u}_h^+)$

For  $\mathbf{v}_h : [d\mathbf{u}_h^-/d\mathbf{u}_h^+] \mathbf{v}_h = 0$ , the terms multiplying  $\mathbf{v}_h$  over  $\partial\kappa \cap \partial\Omega$  are the generally non-zero contributions  $[\partial \mathcal{H}_{\text{bd}}/\partial \mathbf{u}_h^+]^T \boldsymbol{\psi}_h^+$  on the LHS and  $dJ_h(\mathbf{u}_h^+)/d\mathbf{u}_h^+$  on the RHS. Hence the conclusion is also that if  $[d\mathbf{u}_h^-/d\mathbf{u}_h^+]$  has a nonempty null-space, this formulation attempts to introduce adjoint BC's not present in the corresponding PDE problem.

Shown in Figure 1 are the first component of adjoint state  $\boldsymbol{\psi}_h^1$ , for the NACA0012 airfoil, Euler flow test case ( $\alpha = 0^\circ$ ,  $M_\infty = 0.5$ ), with a  $p = 3$ , 6214 elements DG discretization. The upper plot shows the discrete adjoint with consistent boundary flux and output, taken to depend only on the constructed state. In the lower plot, the Roe averaged flux is used, and the drag output depends on the interior state. This dependence on the boundary state is the same as that used by Hartmann and Houston.<sup>8</sup>



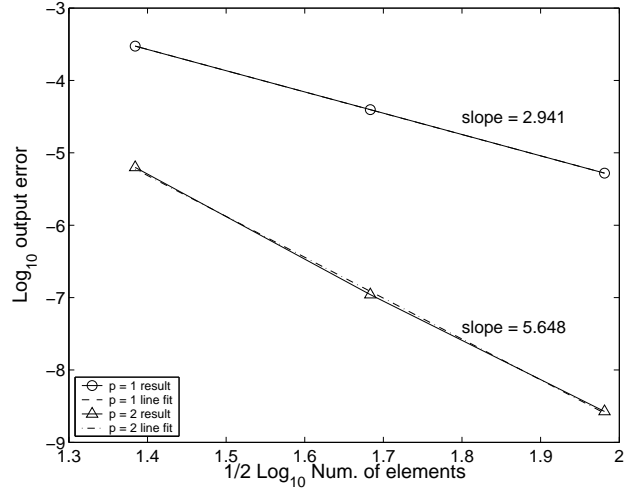
a)  $\mathcal{H}_{bd} = \mathcal{F}(\mathbf{u}_h^-)$ , drag output =  $J_h(\mathbf{u}_h^-)$



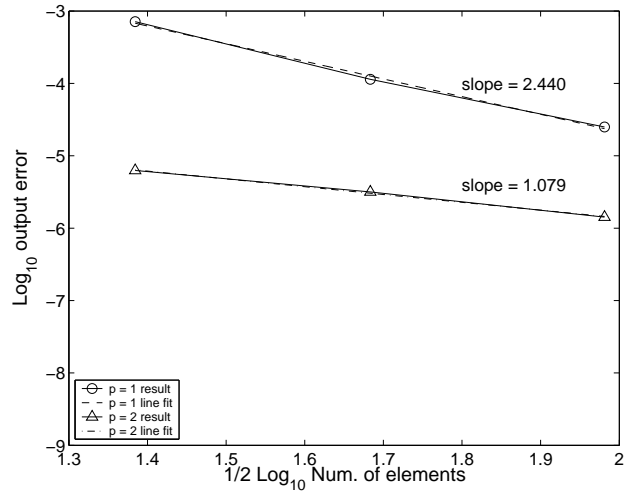
b)  $\mathcal{H}_{bd} = \mathcal{H}_{Roe}(\mathbf{u}_h^+, \mathbf{u}_h^-)$ , drag output =  $J_h(\mathbf{u}_h^+)$

**Fig. 1 Comparison of discrete adjoint solutions for NACA0012 test case.**

The dependence of the boundary flux and output on the constructed/interior states also affects the output grid convergence. By construction, the Galerkin statement for  $\mathbf{u}_h \in \mathcal{V}_h^p$  ensures that the flow residual is orthogonal to all adjoint approximations lying in  $\mathcal{V}_h^p$ . This property ensures output superconvergence if the error  $\mathbf{u} - \mathbf{u}_h$  satisfies the homogeneous Dirichlet boundary condition. However, in general there is a non-zero boundary flux error on  $\partial\Omega$ . The inner product of the boundary flux error and the adjoint solution over  $\partial\Omega$  would constitute a non-zero output error contribution,



a)  $\mathcal{H}_{bd} = \mathcal{F}(\mathbf{u}_h^-)$ , lift output =  $J_h(\mathbf{u}_h^-)$



b)  $\mathcal{H}_{bd} = \mathcal{H}_{Roe}(\mathbf{u}_h^+, \mathbf{u}_h^-)$ , lift output =  $J_h(\mathbf{u}_h^+)$

**Fig. 2 Comparison of output convergence for Gaussian bump test case.**

unless this is a term that is explicitly made to vanish in the definition of the adjoint BC. Hence, if the flow BC is not imposed in a variationally consistent manner, natural output superconvergence could be lost. This conclusion is analogous to the need for a conservative output evaluation in the finite volume context.<sup>10,11</sup> To examine this effect, the lift output convergence is evaluated for a smooth test case of  $M_\infty = 0.5$  compressible flow over a Gaussian bump, on grids with 587, 2327 and 9171 elements using  $p = 1, 2$  solution orders. The truth lift output is taken to be the computed value on the 9171 elements grid using a  $p = 3$  solution order. Figure 2 shows that while the top plot shows the  $2p+1$  superconvergence, the lower plot shows degraded convergence, especially for the  $p = 2$  solution.

### Concurrent flow-adjoint solve

The exact dual adjoint solution algorithm<sup>12,13</sup> is based on the principle of extending an existing flow

iteration algorithm to the adjoint problem by requiring the preservation of linear duality at every iteration. Let

$$\mathbf{L}\mathbf{u} = \mathbf{f} \quad (7)$$

denote the linearized flow (primal) system of equations, with the primal output being

$$\mathcal{J}^{\text{pr}}(\mathbf{u}) = \langle \mathbf{g}, \mathbf{u} \rangle, \quad (8)$$

where  $\langle \cdot, \cdot \rangle$  denotes the Euclidean inner product. Then the corresponding adjoint (dual) problem is

$$\mathbf{L}^T \boldsymbol{\psi} = \mathbf{g}, \quad (9)$$

with the corresponding output

$$\mathcal{J}^{\text{du}}(\boldsymbol{\psi}) = \langle \mathbf{f}, \boldsymbol{\psi} \rangle. \quad (10)$$

For  $\mathbf{u}$ ,  $\boldsymbol{\psi}$  satisfying (7), (9), the outputs are equivalent,

$$\mathcal{J}^{\text{pr}}(\mathbf{u}) = \mathcal{J}^{\text{du}}(\boldsymbol{\psi}). \quad (11)$$

It is desirable to extend the above equivalence to an algorithm level, where approximate solutions to (7) and (9) are obtained in an iterative manner. Denoting  $\mathbf{P}_n$  to be the linear operator that describes  $n$  iterations of the linear flow iteration acting on the flow forcing vector,  $\mathbf{f} \in \mathbb{R}^m$ , so that  $\mathbf{u}_n = \mathbf{P}_n \mathbf{f}$ . Then the exact dual algorithm for the adjoint gives iterates  $\boldsymbol{\psi}_n = \mathbf{P}_n^* \mathbf{g}$  where  $\mathbf{P}_n^*$  is the operator defined to satisfy the following duality property :

$$\langle \mathbf{u}, \mathbf{P}_n \mathbf{v} \rangle = \langle \mathbf{P}_n^* \mathbf{u}, \mathbf{v} \rangle, \quad \forall \mathbf{u}, \mathbf{v} \in \mathbb{R}^m. \quad (12)$$

For  $\mathbf{P}_n^*$  which satisfy (12), the equivalence of outputs is guaranteed at every iteration,

$$\mathcal{J}^{\text{pr}}(\mathbf{u}_n) = \mathcal{J}^{\text{du}}(\boldsymbol{\psi}_n). \quad (13)$$

The adaptive precision optimization we propose requires an estimate of the adjoint during the solution of the primal problem. To obtain this, we concurrently iterate the dual solution with the primal problem. As the nonlinear primal is evolving, the dual system of equations is changing at every iteration. While this might seem to imply a loss of computational efficiency versus the typical sequential calculation of the adjoint from a stationary primal, the concurrent approach has several advantages. In practice, for large-scale problems, the linear system of dual equations cannot be stored and must be recomputed during the dual iterations. However, as this linearization is already

constructed as part of the primal iterations, the adjoint can be iterated at very little extra work during the primal solutions. Furthermore, the adjoint convergence behavior for the concurrent solve is nearly identical to that of the sequential solution.

An adjoint solution algorithm dual to the line-implicit solver described by Fidkowski and Darmofal<sup>7</sup> has been implemented. In our implementation of the concurrent line-implicit flow-adjoint solver, the factors allowing for memory/CPU efficient solves are:

- Fixed, nearest neighbour stencil in DG discretization for all orders. The adjoint residual may then be calculated by looping through all the edges and elements in the grid in a similar manner to the calculation of flow residual.
- Use of LU decomposed matrices to solve for both the linear flow system and the transposed adjoint problem. Hence, line decomposition only needs to be performed once in the concurrent solve for the flow and adjoint updates.

In the flow residual and Jacobian calculation, the numerical flux  $\mathcal{H}(\mathbf{u}_n^+, \mathbf{u}_n^-, \hat{\mathbf{n}})$  together with its linearization at the current state  $\mathbf{u}_n$ ,  $\frac{\partial \mathcal{H}}{\partial \mathbf{u}_n^+}$ ,  $\frac{\partial \mathcal{H}}{\partial \mathbf{u}_n^-}$  is computed at the quadrature points. Similarly for the interior flux  $\mathbf{F}^x(\mathbf{u}_n)$ ,  $\mathbf{F}^y(\mathbf{u}_n)$ . Making use of the readily available linearizations, the adjoint residual is computed as well. That is, in the same quadrature loop performed for each of the interior faces, where the term  $+\mathcal{H}$  and  $-\mathcal{H}$  are added to the left and right pieces of the flow residual,  $[\partial \mathcal{H} / \partial \mathbf{u}_n^+]^T (\boldsymbol{\psi}_n^+ - \boldsymbol{\psi}_n^-)$  and  $-[\partial \mathcal{H} / \partial \mathbf{u}_n^-]^T (\boldsymbol{\psi}_n^- - \boldsymbol{\psi}_n^+)$  are added to the left and right pieces of the adjoint residual. For the interior residuals, in the quadrature sum where the term  $[\mathbf{F}^x, \mathbf{F}^y] \cdot \nabla \mathbf{v}_h$  is added to the flow residual,  $\partial_x \boldsymbol{\psi}_n$ ,  $\partial_y \boldsymbol{\psi}_n$  are computed, multiplied by  $[d\mathbf{F}^x / d\mathbf{u}_n]^T$  and  $[d\mathbf{F}^y / d\mathbf{u}_n]^T$  respectively and added to the adjoint residual.

In the flow line-solve, an  $LU$  decomposition with row pivoting of the block diagonal matrices  $\mathbf{A}$  is performed,

$$\mathbf{P}\mathbf{A} = \mathbf{L}\mathbf{U}. \quad (14)$$

In terms of the above decomposition,  $\mathbf{A}^T$  may be written as

$$\mathbf{A}^T = \mathbf{U}^T \mathbf{L}^T \mathbf{P}. \quad (15)$$

Therefore, a solve for the dual block-diagonal system  $\mathbf{A}^T \mathbf{y} = \mathbf{g}$  involves the following steps:  $\mathbf{U}^T \mathbf{z} = \mathbf{g}$ ,  $\mathbf{L}^T \tilde{\mathbf{y}} = \mathbf{z}$  and finally filling in the entries of  $\mathbf{y}$  from that of  $\tilde{\mathbf{y}}$  using  $\mathbf{P}\tilde{\mathbf{y}} = \mathbf{y}$ .

Table 1 shows the additional CPU time needed for concurrent flow-adjoint solve over the baseline line-implicit solver (with the storage of full flow Jacobian),

for an Euler flow problem with a grid of 9171 elements. Whereas for the sequential approach the adjoint residual computation may be sped up by storing the transposed Jacobian (or part thereof) if large memory is available,<sup>13</sup> for the concurrent approach this is no longer possible. However, utilizing the linearization already performed in the flow residual/Jacobian calculation also results in CPU savings with no extra memory.

**Table 1 Concurrent flow-adjoint**

Solution order	Additional CPU time
$p = 0$	40.7 %
$p = 1$	35.1 %
$p = 2$	33.4 %
$p = 3$	23.2 %

We now develop an output error estimate due to iteration using the concurrent iterates  $\mathbf{u}_n$  and  $\boldsymbol{\psi}_n$ . For approximate solutions  $\mathbf{u}_n, \boldsymbol{\psi}_n$  to the linear primal and dual systems (7), (9), one has following error expansion for the output:

$$\mathcal{J}^{\text{pr}}(\mathbf{u}) - \mathcal{J}^{\text{pr}}(\mathbf{u}_n) = \langle \mathbf{R}_n^{\text{pr}}, \boldsymbol{\psi}_n \rangle + \langle \mathbf{R}_n^{\text{pr}}, \mathbf{L}^{-T} \mathbf{R}_n^{\text{du}} \rangle, \quad (16)$$

where the primal and adjoint algebraic residuals are defined as  $\mathbf{R}_n^{\text{pr}} \equiv \mathbf{f} - \mathbf{L}\mathbf{u}_n$ ,  $\mathbf{R}_n^{\text{du}} \equiv \mathbf{g} - \mathbf{L}^T \boldsymbol{\psi}_n$ . Hence, denoting the smallest singular value of  $\mathbf{L}$  by  $\sigma_{\min}$ , one has the following bound:

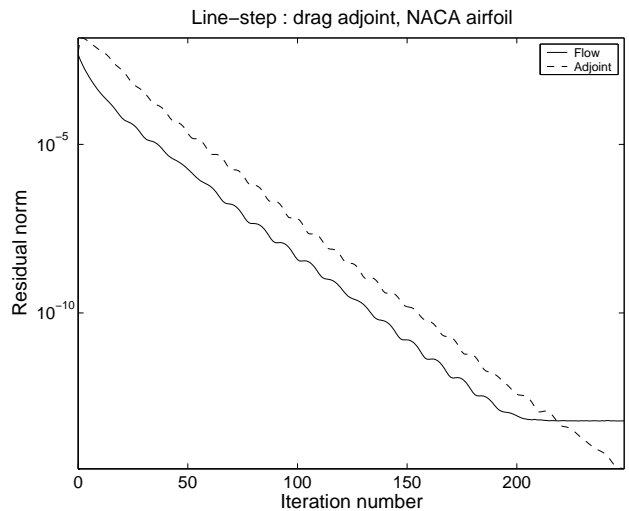
$$|\mathcal{J}^{\text{pr}}(\mathbf{u}) - \mathcal{J}^{\text{pr}}(\mathbf{u}_n)| \leq |\langle \mathbf{R}_n^{\text{pr}}, \boldsymbol{\psi}_n \rangle| + \frac{\|\mathbf{R}_n^{\text{pr}}\| \|\mathbf{R}_n^{\text{du}}\|}{\sigma_{\min}}. \quad (17)$$

The above shows that if  $\|\mathbf{R}_n^{\text{du}}\| \rightarrow 0$  at the same rate as the primal residual, the dominant term contributing to the primal output iterative error is  $|\langle \mathbf{R}_n^{\text{pr}}, \boldsymbol{\psi}_n \rangle|$ . Hence, this computable term can be used as an iterative error estimate. Using it as an output error correction, the resulting output convergence can be doubled that of the primal residual.

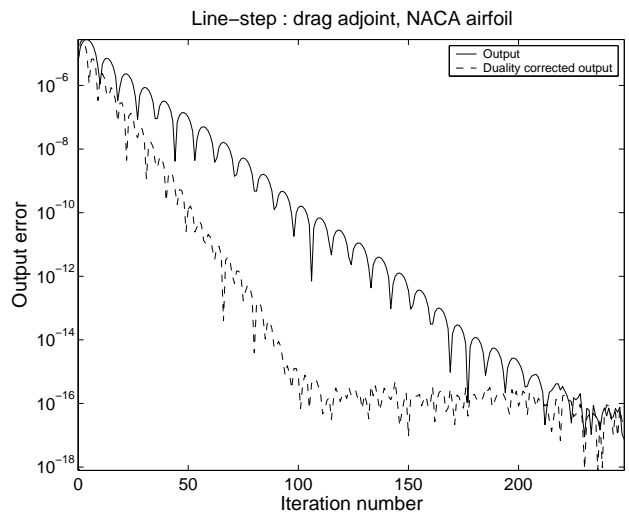
Figure 3 shows the residuals and drag output convergence for a  $p = 3$ , 6494 elements DG discretization of the Euler compressible flow equations around a NACA0012 airfoil at  $0^\circ$  angles of attack with free-stream Mach number  $M_\infty = 0.5$ . The flow and adjoint residual show the same convergence behavior, as is to be expected. The result shows that, in the nonlinear setting, the adjoint correction term results in the doubled output convergence rate. Using this term as an iterative error estimate, the corresponding effectivity can be seen to quickly converge and stay close to 1, until the output has converged to within very small error of  $10^{-14}$ .

### Adaptive precision methodology

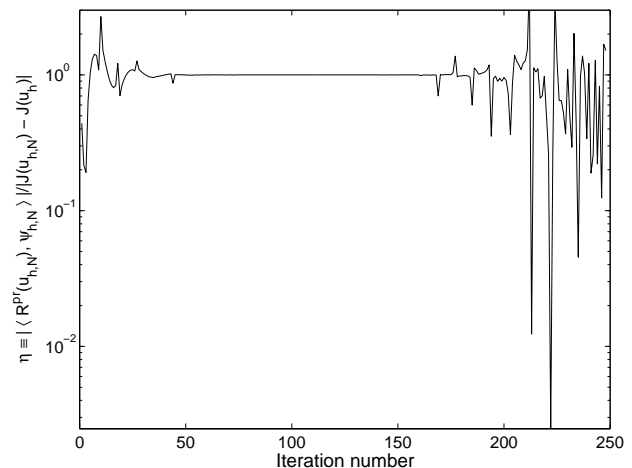
Recently, steps have been taken towards grid refinement within the optimization loop and partial con-



a) Residual convergence.



b) Output convergence.



c) Effectivity of iterative error estimate.

**Fig. 3 Concurrent solve convergence.**

vergence of flow and adjoint equations on each of the successive grids. In particular, in a series of papers, Dadone and Grossman<sup>14-16</sup> have arrived at a methodology for partially converging the flow and adjoint approximations on progressively (uniformly) refined grids and a modified steepest descent to take into account the use of approximate gradients provided by the partially converged adjoints. The methodology results in orders of magnitude computational time savings for a wide class of aerodynamic problems.

Provably convergent algorithm models for performing grid refinement within the optimization loop have been derived and demonstrated by Polak and co-workers.<sup>1,17,18</sup> Conceptually, an infinite sequence of *epi-converging* approximations  $\mathbf{P}_k$  to an unimplementable optimization problem  $\mathbf{P}$  is considered. For example, the  $\mathbf{P}_k$  may be a sequence of finite-element optimization problems with decreasing grid-size parameter  $h$ , which approximate the PDE optimization problem  $\mathbf{P}$  in the limit. For each  $\mathbf{P}_k$ , a traditional optimization algorithm would produce a sequence of control iterates. Appropriately organizing the calculations so that the next approximation in the hierarchy of optimization problems is used when certain refinement criteria are satisfied, the sequence of iterates obtained is ensured to converge to a stationary point of  $\mathbf{P}$ . Recently, the algorithm models have been extended to the case where the refinement decisions control both the discretization and iteration parameters,  $h$  and  $N$ .<sup>2</sup> For flow optimization problems, Pironneau et al show that the methodology can result in an order of magnitude saving in the computation time.<sup>2,19</sup>

Denote the approximate objective function at the discretized control  $\mathbf{d}_h$  by  $\mathcal{J}(\mathbf{u}_{h,N}, \mathbf{d}_h)$ , where  $\mathbf{u}_{h,N} = \mathbf{u}_{h,N}(\mathbf{d}_h)$  is assumed in the notation. In the paper of Pironneau and Polak, it is assumed that positive functions  $\Delta(h), \varphi(h, N), N^*(h)$  are known *a priori*, with the following limiting convergence properties,<sup>2</sup>

$$\begin{aligned} \lim_{h \rightarrow 0} \Delta(h) &= 0, \\ \lim_{N \rightarrow \infty} \varphi(h, N) &= 0, \quad \forall h > 0, \\ \lim_{h \rightarrow 0} \varphi(h, N) &= 0, \quad \forall N > N^*(h). \end{aligned} \quad (18)$$

Furthermore,  $\Delta(h), \varphi(h, N)$  are error bounding functions for  $\mathcal{J}$  in the following sense: for all bounded controls  $\mathbf{d}_h$  in a finite dimensional space  $\mathcal{D}_h$ ,

$$|\mathcal{J}(\mathbf{u}_h, \mathbf{d}_h) - \mathcal{J}(\mathbf{u}, \mathbf{d}_h)| \leq \xi \Delta(h), \quad \forall h \in (0, h_{max}],$$

$$|\mathcal{J}(\mathbf{u}_{h,N}, \mathbf{d}_h) - \mathcal{J}(\mathbf{u}_h, \mathbf{d}_h)| \leq \xi \varphi(h, N), \quad \forall h \in (0, h_{max}], \quad \text{Set } \mathbf{u}_h \rightarrow \mathbf{u}_{h,N}, \psi_h \rightarrow \psi_{h,N}.$$

for some appropriately small  $h_{max}$  and bounded constant  $\xi < \infty$ . For application to the optimization of finite element discretizations of PDEs on a domain

$\Omega = \Omega(\mathbf{d}_h)$ , there exist an *a posteriori* error representation for the output, of the form

$$|\mathcal{J}(\mathbf{u}_h, \mathbf{d}_h) - \mathcal{J}(\mathbf{u}, \mathbf{d}_h)| \approx |\mathcal{E}_\Omega(\mathbf{u}_h; \psi - \psi_h)|. \quad (19)$$

In our work, the output error estimate for the DG discretization is obtained by estimating the state and adjoint error  $\mathbf{u} - \mathbf{u}_h, \psi - \psi_h$  via interpolation and using the DG semilinear form  $\sum_\kappa B_\kappa(\cdot, \cdot)$ ,<sup>4</sup>

$$\mathcal{E}_\Omega(\mathbf{u}_h; \psi - \psi_h) = \sum_\kappa B_\kappa(\mathbf{u} - \mathbf{u}_h, \psi - \psi_h). \quad (20)$$

Since the above is readily available as a product of the error estimation procedure performed for the output-based grid adaptation,<sup>11,20</sup> an attractive alternative to deriving a priori bound function  $\Delta(h)$  is to use (20). Similarly, for the incompletely iterated approximation to a nonlinear system of equations  $\mathbf{R}^{\text{pr}}(\mathbf{u}_h) = 0$ , the output error is, to first order in  $N$ ,

$$|\mathcal{J}(\mathbf{u}_{h,N}, \mathbf{d}_h) - \mathcal{J}(\mathbf{u}_h, \mathbf{d}_h)| \approx |\langle \mathbf{R}^{\text{pr}}(\mathbf{u}_{h,N}), \psi_{h,N} \rangle|.$$

Hence if adjoint estimates  $\psi_{h,N}$  are available, an alternative to heuristically determined  $\varphi(h, N)$  is to use the above estimate:  $\varphi(h, N) = |\langle \mathbf{R}^{\text{pr}}(\mathbf{u}_{h,N}), \psi_{h,N} \rangle|$ . For the function  $N^*(h)$ , a choice that satisfies the last line of (18) is to define it to be the smallest  $N$  such that the iterative error is less than a certain  $\zeta$  multiple of the discretization error:

$$\arg \min_N : |\langle \mathbf{R}^{\text{pr}}(\mathbf{u}_{h,N}), \psi_{h,N} \rangle| \leq \zeta |\mathcal{E}_\Omega(\mathbf{u}_h; \psi - \psi_h)|.$$

In practice,  $\mathbf{u}_h$  and  $\psi_h$  of the RHS of the above can only be approximated by  $\mathbf{u}_{h,N}, \psi_{h,N}$ . Hence a further assumption is that the discretization error can be well-estimated using the incompletely iterated approximations. Let  $\mathbf{d}_h \rightarrow A_h(\mathbf{d}_h, \mathbf{u}_{h,N}, \psi_{h,N})$  denote a general gradient-based optimization algorithm for finite dimensional inputs  $\mathbf{d}_h$  and  $\text{AdaptGrid}(\text{FF}, \mathbf{d}_h, \mathbf{u}_{h,N}, \psi_{h,N})$  denote an output-based grid adaptation algorithm that refines the degrees of freedoms by a certain fixed fraction, FF. Using the a posteriori output estimates in the precision tests, the proposed methodology is a modification of the Algorithm Model 2 proposed by Pironneau and Polak,<sup>2</sup> taking positive scalars  $\gamma, \zeta$  and  $\tau$  as inputs.

#### Adaptive Precision Algorithm ( $\gamma, \zeta, \tau, \text{FF}$ )

Initial control:  $\mathbf{d}_h \in \mathcal{D}_h$ .

Initial converged solution:  $\mathbf{u}_h, \psi_h$ .

Set  $\mathbf{u}_h \rightarrow \mathbf{u}_{h,N}, \psi_h \rightarrow \psi_{h,N}$ .

#### Begin Outer Loop

While Inner Loop: counter  $j = 0, 1, \dots, j_{max}$

1. Obtain estimate  $\Delta(h) = |\mathcal{E}_\Omega(\mathbf{u}_{h,N}; \boldsymbol{\psi} - \boldsymbol{\psi}_{h,N})|$ .
2. Compute control update

$$\tilde{\mathbf{d}}_h = A_h(\mathbf{d}_h, \mathbf{u}_{h,N}, \boldsymbol{\psi}_{h,N}). \quad (21)$$

3. Iterate state updates  $\tilde{\mathbf{u}}_{h,N}, \tilde{\boldsymbol{\psi}}_{h,N}$  until:

$$|\langle \mathbf{R}^{\text{Pr}}(\tilde{\mathbf{u}}_{h,N}), \tilde{\boldsymbol{\psi}}_{h,N} \rangle| \leq \zeta \tau^j \Delta(h). \quad (22)$$

4. Set  $\varphi(h, N) = |\langle \mathbf{R}^{\text{Pr}}(\tilde{\mathbf{u}}_{h,N}), \tilde{\boldsymbol{\psi}}_{h,N} \rangle|$ .

5. If  $\mathcal{J}(\tilde{\mathbf{u}}_{h,N}, \tilde{\mathbf{d}}_h) - \mathcal{J}(\mathbf{u}_{h,N}, \mathbf{d}_h) < -\varphi(h, N)$  exit **Inner Loop**.

Else Iterate  $\mathbf{u}_{h,N}, \boldsymbol{\psi}_{h,N}$  until:

$$|\langle \mathbf{R}^{\text{Pr}}(\mathbf{u}_{h,N}), \boldsymbol{\psi}_{h,N} \rangle| \leq \zeta \tau^{j+1} \Delta(h). \quad (23)$$

### End Inner Loop

- Set

$$\hat{\Delta}(h, N) = \Delta(h) + \varphi(h, N).$$

- If  $\mathcal{J}(\tilde{\mathbf{u}}_{h,N}, \tilde{\mathbf{d}}_h) - \mathcal{J}(\mathbf{u}_{h,N}, \mathbf{d}_h) > -\gamma \hat{\Delta}(h, N)$ , call **AdaptGrid**(FF,  $\mathbf{d}_h, \mathbf{u}_{h,N}, \boldsymbol{\psi}_{h,N}$ ), go to **Inner Loop**.

Else Update control and states :

$$\{\tilde{\mathbf{d}}_h; \tilde{\mathbf{u}}_{h,N}; \tilde{\boldsymbol{\psi}}_{h,N}\} \rightarrow \{\mathbf{d}_h; \mathbf{u}_{h,N}; \boldsymbol{\psi}_{h,N}\}. \quad (24)$$

### End Outer Loop

In the inner loop, the iterative error is initially made to be less than a  $\zeta$  multiple of the discretization error. If the change in the approximate objective function is not sufficiently negative (as may be the case if the approximate gradient obtained from the partially converged adjoint does not result in a descent direction), additional iteration as governed by  $\tau$  is performed. If the discrete (rather than the continuous) adjoint formulation is used in the computation of gradient, the completely converged gradient is assured to result in a descent direction; hence for all  $h$  the inner loop will terminate at some finite  $N$ . Otherwise, a maximum  $j_{max}$  has to be enforced on the inner loop in order to exit and refine  $h$  where necessary. In the outer loop, the refinement test ensures that the  $h$  parameter decreases to zero if the sequence of controls has an accumulation point. If  $\gamma > 1$ , the discretization error is controlled to be less than the approximate objective function change, thus ensuring monotonic convergence of the objective values evaluated on the “truth” grid using the controls obtained from the adaptive precision algorithm.

For the proposed algorithm, a question of interest is determining the range of the parameters  $\gamma, \zeta$  that would be the most efficient. Let  $\mathbf{d}^*$  denote the true

optimizer for the objective function  $\mathcal{J}(\mathbf{u}(\cdot), \cdot)$  and the corresponding flow solution  $\mathbf{u}^* \equiv \mathbf{u}(\mathbf{d}^*)$ . In certain applications, an ultimate goal of the optimization computation may be obtaining the value  $\mathcal{J}(\mathbf{u}^*, \mathbf{d}^*)$ , the minimum cost attainable in a certain design space. In any case, it may be useful to consider the difference between  $\mathcal{J}(\mathbf{u}_{h,N}, \mathbf{d}_h)$  and  $\mathcal{J}(\mathbf{u}^*, \mathbf{d}^*)$  as the quantity to be controlled in the adaptive process. This may be written as,

$$\begin{aligned} & |\mathcal{J}(\mathbf{u}_{h,N}, \mathbf{d}_h) - \mathcal{J}(\mathbf{u}^*, \mathbf{d}^*)| \\ & \leq |\mathcal{J}(\mathbf{u}_{h,N}, \mathbf{d}_h) - \mathcal{J}(\mathbf{u}_{h,N}, \mathbf{d}^*)| \\ & \quad + |\mathcal{J}(\mathbf{u}_h, \mathbf{d}^*) - \mathcal{J}(\mathbf{u}^*, \mathbf{d}^*)| \\ & \quad + |\mathcal{J}(\mathbf{u}_{h,N}, \mathbf{d}^*) - \mathcal{J}(\mathbf{u}_h, \mathbf{d}^*)| \\ & \approx |\mathcal{J}(\mathbf{u}_{h,N}, \mathbf{d}_h) - \mathcal{J}(\mathbf{u}_{h,N}, \mathbf{d}^*)| \\ & \quad + |\mathcal{J}(\mathbf{u}_h, \mathbf{d}_h) - \mathcal{J}(\mathbf{u}, \mathbf{d}_h)| \\ & \quad + |\mathcal{J}(\mathbf{u}_{h,N}, \mathbf{d}_h) - \mathcal{J}(\mathbf{u}_h, \mathbf{d}_h)|. \end{aligned} \quad (25)$$

The above shows that the LHS term is bounded by three terms whose magnitudes can be controlled by the optimizer, discretization and iteration refinement respectively. If the computational processes of optimization, grid refinement, and iterative solution were independent of each other, a good strategy would be to choose the control that leads to maximum error decrease per unit computational cost. However, this is not the case as refining the grid will drive up the cost of each subsequent solution iteration, which in turn affects the cost of each optimization step. Ideally, the parameters  $\gamma$  and  $\zeta$  should be chosen so that a decreasing number of optimization and solution iterations are performed on increasingly refined grids. If  $\gamma$  is chosen significantly larger than 1 the discretization error is made unnecessarily small compared to the changes given by the optimizer, resulting in an inefficient strategy. The parameter  $\zeta$  should be set so that the iteration error is controlled to be less than the discretization error. For robustness and efficiency, it is reasonable to set  $\zeta$  an order of magnitude or two smaller than 1, but not much less.

## Quasi-one dimensional flow

The quasi-one dimensional Euler equations for an inviscid, compressible flow in a shape-varying nozzle normalized to the unit interval may be written in the form,

$$\frac{d\mathcal{F}(\mathbf{u}, A)}{dx} - \mathcal{G}(\mathbf{u}, A) = 0, \quad x \in [0, 1], \quad (26)$$

where  $A$  denotes the nozzle area and

$$\mathcal{F}(\mathbf{u}, A) \equiv \begin{pmatrix} \rho u A \\ (\rho u^2 + p) A \\ \rho u H A \end{pmatrix},$$

$$\mathcal{G}(\mathbf{u}, A) \equiv \begin{pmatrix} 0 \\ p \frac{dA}{dx} \\ 0 \end{pmatrix}, \quad (27)$$

where  $H$  is the total enthalpy. As boundary conditions, the total temperature and pressure  $T_t, p_t$  are imposed at the inlet, the back pressure  $p_B$  at the outlet. For the work shown here, the  $p = 1$  DG discretization is used. The inverse-design type objective function used is of the form,

$$\mathcal{J}(\mathbf{u}, \mathbf{d}_h) = \int_0^1 [p(\mathbf{u}) - p_{spec}]^2 dx, \quad (28)$$

where  $\mathbf{u}$  is the state,  $\mathbf{d}_h$  the controls and  $p_{spec}$  is a given 6th degree polynomial pressure distribution. We work in a 10 dimensional design space of polynomial-shaped nozzles of degrees  $< 10$ . The design parameters  $\mathbf{d}_h = \{\alpha_0, \alpha_1, \dots, \alpha_9\}$  are the polynomial coefficients of the nozzle shape,  $A(x, \mathbf{d}_h) = \alpha_9 x^9 + \alpha_8 x^8 + \dots + \alpha_0$ .

The concurrent flow-adjoint solve uses the backwards Euler iteration, with a fixed CFL = 100. The state and adjoint error  $\mathbf{u} - \mathbf{u}_h, \psi - \psi_h$  are estimated via interpolation to obtain output error estimates as given in (20). The elemental contribution  $|B_{\kappa}(\mathbf{u} - \mathbf{u}_h|_{\kappa}, \psi - \psi_h|_{\kappa})|$  serves as a local error indicator, which can then be used in a output-based grid adaptation strategy. In the current work, the grid is modified using the fixed fraction strategy, where the 1/4 proportion of elements with the most error contribution are refined. The optimizer used is the method of gradient descent with polynomial model stepsize control.<sup>21</sup> The parameter  $\tau = 1/3$  is chosen for all the results shown. Also, as a safeguard, a minimal number of 2 solution iterations is imposed. Figure 4 shows the initial, final pressure distributions and nozzle shapes. For the choicen optimizer and design parameters, a relatively large number of  $\sim 600$  design iterations are needed to reach convergence. Clearly, this can be improved by using better optimizers and different shape parametrizations. However this is not crucial for our current purpose of demonstrating the general behavior of adaptive optimization.

Figure 5 shows the computational result for parameters  $\gamma = 1, \zeta = 0.001$ . The discretization control parameter is reasonably chosen, but the iteration error is controlled to be very small. It is observed that on coarse grids, few iterations are necessary despite the stringent control. On finer grids, decreasing number of solution iterations are needed as optimization proceeds.

Figure 6 shows the result for  $\gamma = 1$  as previously but with a more reasonable choice of the iteration pa-

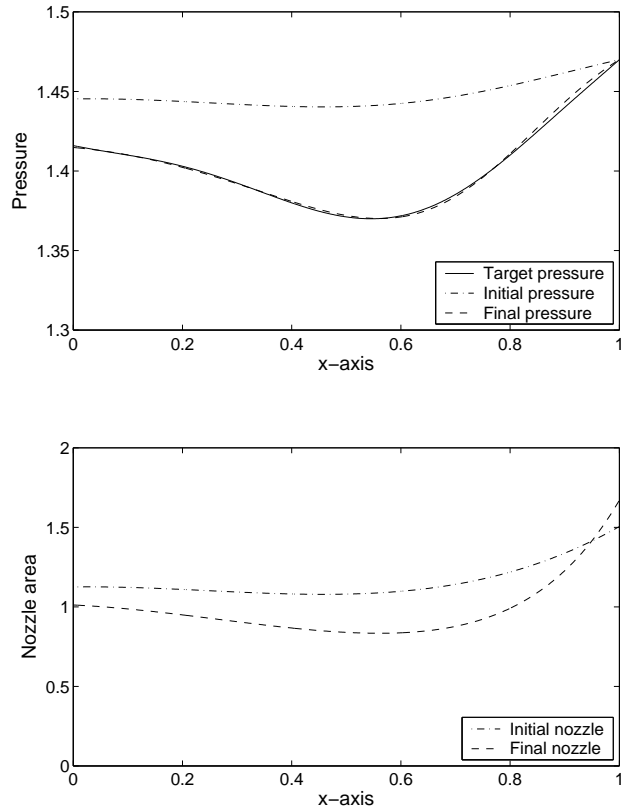


Fig. 4 Nozzle inverse design.

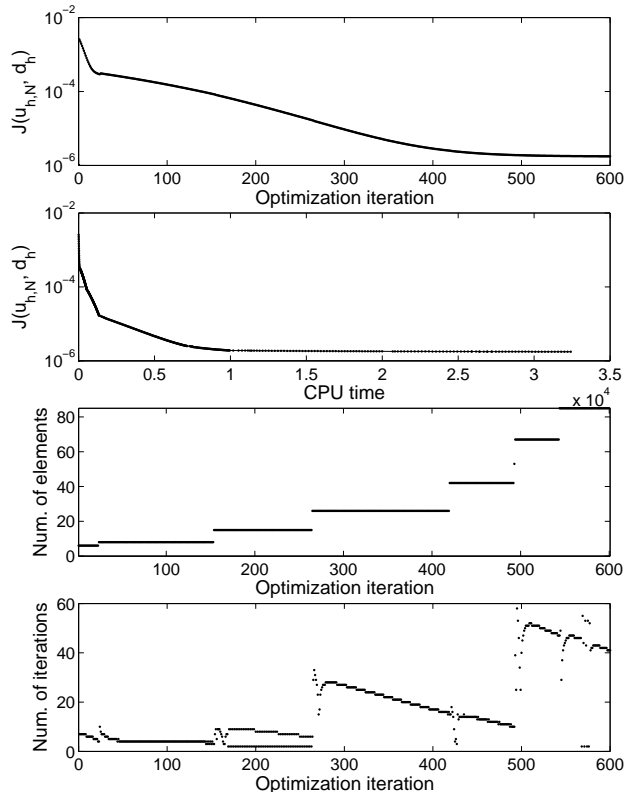
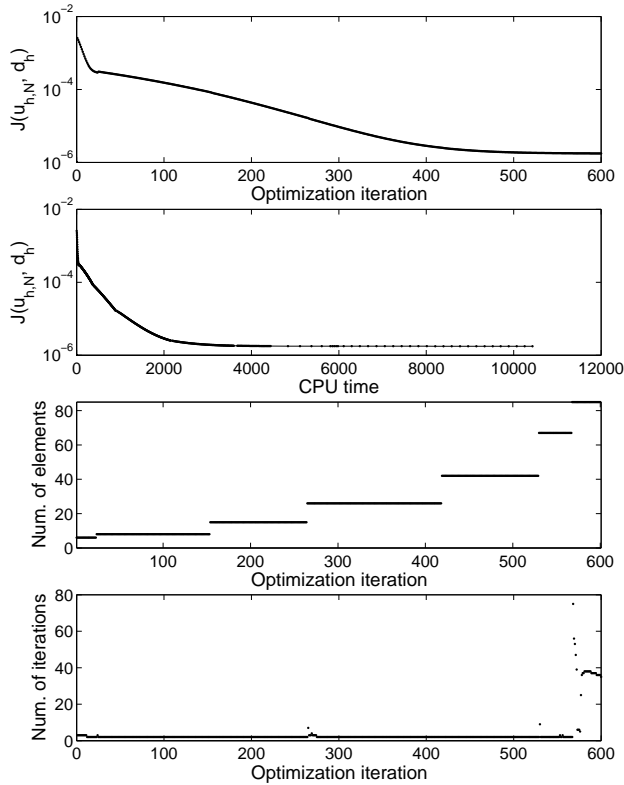


Fig. 5 Adaptive precision:  $\gamma = 1, \zeta = 0.001$



**Fig. 6 Adaptive precision:**  $\gamma = 1, \zeta = 0.2$

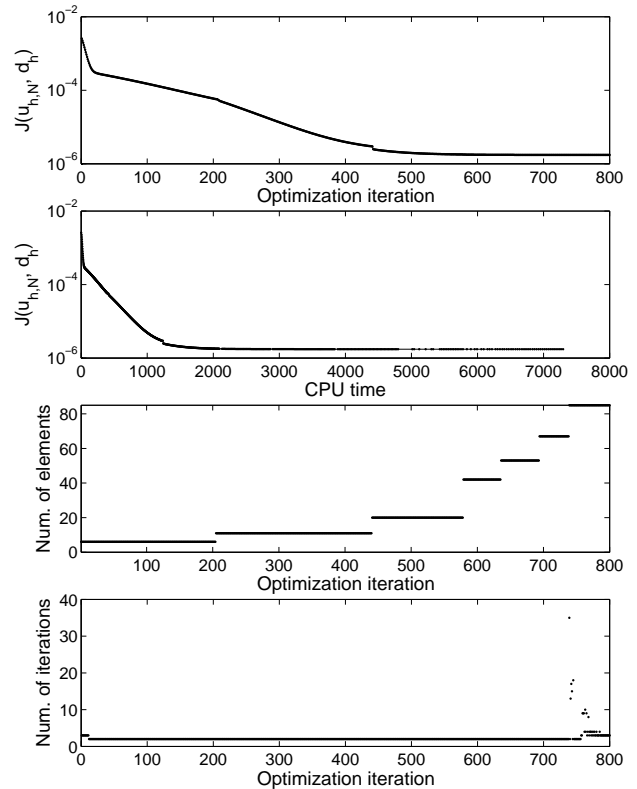
parameter  $\zeta = 0.2$ . Comparison with Figure 5 shows that the choice  $\zeta = 0.001$  is indeed too stringent: the optimization convergence is very similar to the previous case, but requiring much fewer solution iterations overall. Upon grid refinement, initially a larger number of solution iterations is necessary to converge the flow approximation to the output precision criterion. Following that, there is virtually no need to iterate the solution much further. Only on the finest grid is significantly more iterations needed throughout.

Figure 7 shows that decreasing the discretization parameter from  $\gamma = 1$  to  $\gamma = 0.05$  and keeping  $\zeta = 0.2$  results in similar convergence behavior but somewhat improved computational efficiency. Although more optimization iterations were needed to reach convergence, choosing  $\gamma$  smaller than 1 results in increased computational efficiency.

given that grid refinement is an expensive decision it is not unexpected that it is advantageous to choose  $\gamma$  smaller than 1.

Figures 5 and 8 confirm the argument that  $\gamma$  should not be chosen larger than 1 and  $\zeta$  not less than 0.01. Both choices result in a three or four fold increase in computational time over that for  $\gamma = 1, \zeta = 0.2$  and  $\gamma = 0.05, \zeta = 0.2$ .

The adaptive approach is clearly superior to the fixed precision approach, shown in Figure 9. Here the optimization is performed on a fixed, 85 element grid and the flow residual is made to converge to a fixed, low value of  $10^{-10}$ . Although the number of solution itera-



**Fig. 7 Adaptive precision:**  $\gamma = 0.05, \zeta = 0.2$

tions per optimization step decreases as the optimizer converges, the total computational cost is an order of magnitude higher than the best adaptive cases.

## Concluding Remarks

Discretization and iteration error estimates are applied to a provably convergent algorithm model for adaptive optimization. Using refinement tests based on a posteriori error estimates eliminates the need to form problem-dependent bound functions with appropriate constants. In the proposed algorithm, two parameters control the relative tolerance of optimization, discretization and iteration. The range of appropriate parameters given by a heuristic argument is consistent with computational results. Finding the most efficient parameters becomes a problem that essentially only depends on the convergence rate of the optimizer used and the scaling of the computational cost with refinement. Preliminary results show that optimization convergence can be controlled in a robust and efficient manner.

## Acknowledgement

This work was supported by NASA Langley Research Center through NASA Grant NAG-1-03035.

## References

- <sup>1</sup>Polak, E., *Optimization : algorithms and consistent approximations*, Springer-Verlag, New York, 1997.

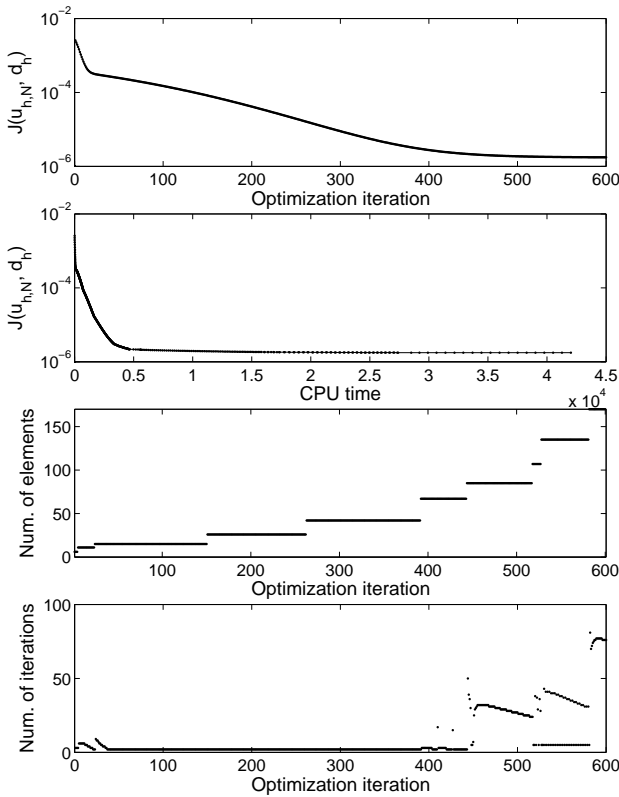


Fig. 8 Adaptive precision:  $\gamma = 10, \zeta = 0.2$

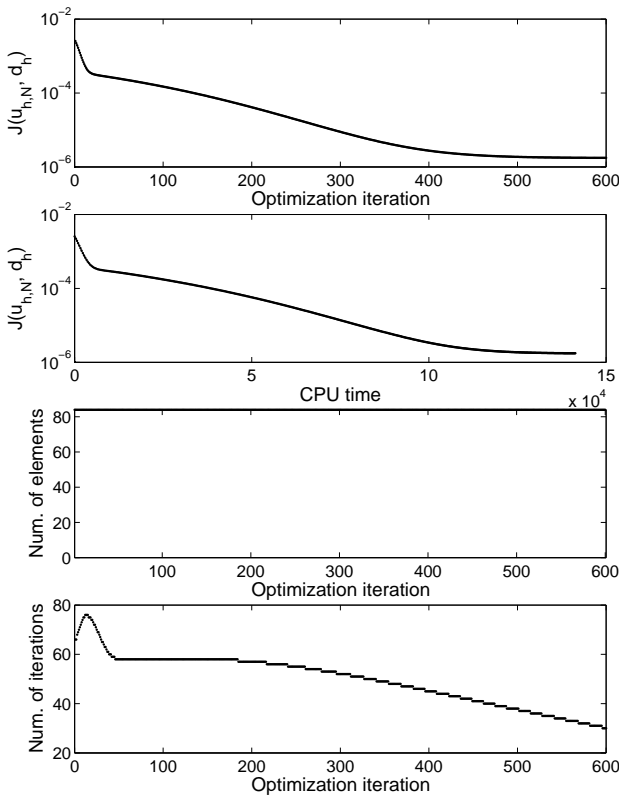


Fig. 9 Fixed precision.

<sup>2</sup>Pironneau, O. and Polak, E., "Consistent approximations and approximate functions and gradients in optimal control," *SIAM Journal on Control and Optimization*, Vol. 41, No. 2, 2002, pp. 487–510.

<sup>3</sup>Barth, T. and Deconinck, H., editors, *Error estimation and adaptive discretization methods in CFD*, Vol. 25 of *Lecture Notes on Computational Science and Engineering*, Springer-Verlag, New York, 2003.

<sup>4</sup>Giles, M. B. and Süli, E., "Adjoint methods for PDEs: a posteriori error analysis and postprocessing by duality," *Acta Numerica*, Vol. 11, 2002, pp. 145–236.

<sup>5</sup>Bassi, F. and Rebay, S., "High-order accurate discontinuous finite element solution of the 2D Euler equations," *Journal of Computational Physics*, Vol. 138, No. 2, 1997, pp. 251–285.

<sup>6</sup>Cockburn, B. and Shu, C.-W., "Runge-Kutta discontinuous Galerkin methods for convection-dominated problems," *Journal of Scientific Computing*, Vol. 16, No. 3, 2001, pp. 173–261.

<sup>7</sup>Fidkowski, K. J. and Darmofal, D. L., "Development of a higher-order solver for aerodynamic applications," AIAA Paper 2004–0436, Jan. 2004.

<sup>8</sup>Hartmann, R. and Houston, P., "Adaptive discontinuous Galerkin finite element methods for the compressible Euler equations," *Journal of Computational Physics*, Vol. 183, No. 2, 2002, pp. 508–532.

<sup>9</sup>Giles, M. B. and Pierce, N. A., "Adjoint equations in CFD: duality, boundary conditions and solution behaviour," AIAA Paper 97-1850, Jan. 1997.

<sup>10</sup>Giles, M. B., Duta, M. C., Muller, J.-D., and Pierce, N. A., "Algorithm developments for discrete adjoint methods," *AIAA Journal*, Vol. 41, No. 2, 2003, pp. 1–32.

<sup>11</sup>Venditti, D. A. and Darmofal, D. L., "Anisotropic grid adaptation for functional outputs : application to two-dimensional viscous flows," *Journal of Computational Physics*, Vol. 187, No. 1, 2003, pp. 22–46.

<sup>12</sup>Giles, M. B., "On the iterative solution of adjoint equations," *Automatic Differentiation: From Simulation to Optimization*, Springer-Verlag, 2001, pp. 145–152.

<sup>13</sup>Nielsen, E., Lu, J., Park, M., and Darmofal, D. L., "An exact dual adjoint solution method for turbulent flows on unstructured grids," AIAA Paper 2003–0272, Jan. 2003.

<sup>14</sup>Dadone, A. and Grossman, B., "Progressive optimization of inverse fluid dynamic design problems," *Computers and Fluids*, Vol. 29, No. 1, 2000, pp. 1–32.

<sup>15</sup>Dadone, A. and Grossman, B., "Fast convergence of viscous airfoil design problems," *AIAA Journal*, Vol. 40, No. 10, 2002, pp. 1997–2005.

<sup>16</sup>Dadone, A. and Grossman, B., "Fast convergence of inviscid fluid dynamic design problems," *Computers and Fluids*, Vol. 32, No. 4, 2003, pp. 607–627.

<sup>17</sup>He, L. and Polak, E., "Effective diagonalization strategies for the solution of a class of optimal design problems," *IEEE Transactions on Automatic Control*, Vol. 35, 1990, pp. 257–267.

<sup>18</sup>Kirjner, C. and Polak, E., "On the use of consistent approximations for the optimal design of beams," *SIAM Journal on Control and Optimization*, Vol. 34, No. 6, 1996, pp. 1891–1913.

<sup>19</sup>Mohammadi, B. and Pironneau, O., *Applied shape optimization for fluids*, Oxford University Press, Oxford, 2001.

<sup>20</sup>Venditti, D. A. and Darmofal, D. L., "Grid adaptation for functional outputs : application to two-dimensional inviscid flows," *Journal of Computational Physics*, Vol. 176, No. 1, 2002, pp. 40–69.

<sup>21</sup>Kelley, C. T., *Iterative methods for optimization*, Society for Industrial and Applied Mathematics, Philadelphia, 1999.